

CHAPTER VI
THERMAL ETCHING OF (10 $\bar{1}$ 0) FACES
OF TELLURIUM SINGLE CRYSTALS

Thermal etching is known to be produced at crystal imperfections, thermally etched dislocation pits and thermal grooves at grain boundaries being examples. Thermal etching has been successfully employed in many crystals like silver¹⁻⁸, some tellurides⁹ and alkali halides^{10,11}.

Divergent views and contradictory results have been reported regarding the utility of this method to reveal dislocation sites. Thermally etched grooves along grain boundaries have been

studied by Chalmers et al.¹. Mullins⁶ gives a general indication that thermal etching can be employed to study dislocations. Moore and others^{3,4} have studied the influence of surface energy on thermal etching without specifically assuming dislocation sites. Studies on individual dislocations in silver crystals have been made by Hendrickson et al.² and Hirth et al.⁵. Hendrickson et al. report that there exists a close agreement between the measured pit density and the theoretical estimate of dislocations in bent crystals. Hirth et al., on the other hand, report that there is no unequivocal agreement between thermal etch pits, since pit densities on $\{100\}$ and $\{110\}$ planes differ largely. A possible explanation for the noncorrespondence may be due to the fact that the formation of etch pits at dislocations is dependent on the components of Burgers vectors normal to the surface. Danilov⁸ studying thermal etch pits on silver crystals at high temperatures explained the existence of pits on the basis of the fact that the evaporation proceeds more intensely than the movement of the atoms over the surface.

Among other metals studied are copper¹²⁻¹⁵, chromium¹⁶, silicon¹⁷, silicon-iron¹⁸, antimony^{19,20} and germanium²¹. Thermal etching has been successfully

employed by Thakkar²⁰ to study the dislocations in antimony. Results of these studies indicate that generally the correspondence between dislocations and etch pits occurs. Etch spirals indicative of screw dislocations have been observed in some cases^{12,14}.

The present work has been taken up to study the correlation between thermal etching and chemical etching and to assess the merits of thermal etching as a means to study dislocations.

Chemical reagents to reveal dislocations in single crystals of tellurium have been reported by many workers²²⁻²⁴. Lovell et al. were the first to report a chemical reagent that produces dislocation pits on cleaved $\{10\bar{1}0\}$ faces of tellurium. The etching was carried out at room temperature. Their etchant contained 3 parts HF, 5 parts HNO₃ and 6 parts acetic acid. Finding that this reagent failed to produce pits on a plane parallel to c-axis Blum²³ used concentrated nitric acid to etch the same face and found that it produced a large number of pits. He also developed a reagent which produced isolated pits on the skull parallel to c-axis.

The etchant was composed of 49 gms H_3PO_4 , 1 cc conc. H_2SO_4 and 5 gms crystalline CrO_3 .

Blakemore et al.²⁴ using hot sulphuric acid produced pits at dislocation sites on $\{10\bar{1}0\}$ cleavage faces of melt-grown Te single crystals. The pits had a very characteristic shape and was found to be assymmetric about the c-axis. Blakemore et al.²⁵ observed two types of pits which were mirror images of each other. This was attributed to the dextro- and laevo-rotary forms of tellurium.

Blakemore et al.²⁴ using optical reflection technique, determined the orientation of the pit faces. On the $(10\bar{1}0)$ observation plane the pit faces were found to correspond to $(1\bar{1}00)$, $(10\bar{1}3)$, $(01\bar{1}1)$ and $(0\bar{1}1\bar{1})$, in the case of laevo-rotary Te single crystal.

Koma et al.²⁶ studied the pits produced by hot sulphuric acid. They have proposed a microscopic model of the etch pit and have shown that the planes constituting a pit are not those suggested by Blakemore et al., but are $(15\bar{6}0)$, $(1\bar{6}51)$, $(\bar{1}8\bar{7}1)$ and $(05\bar{5}1)$ for a left-handed crystal. They concluded that from the nature of the pit the handedness and the positive

directions of the crystal can be determined. They have shown that a crystal with the etch pits as shown in Fig.VI.1a is a right-handed crystal and one with etch pits as in Fig.VI.1b is a left-handed crystal. Their results have been further confirmed by NMR studies.

Shukla²⁷ has made a comparative study of the different etchants reported for Te. He has concluded that of all the chemical reagents reported hot H_2SO_4 is the best to reveal dislocations in Te even though all the pits produced are not at dislocation sites.

Thermal etching of Te has not been reported so far. The comparatively high vapour pressure and the onset of evaporation at low temperatures make the thermal etching studies easier.

Vapour-grown crystals in the form of hexagonal rods, 1.5 to 2 cms in length and 1 to 2 mm² in cross-section, were used for the studies carried out. The as-grown $\{10\bar{1}0\}$ prism planes were etched. The planes were usually smooth and devoid of any growth features, except in a few cases.

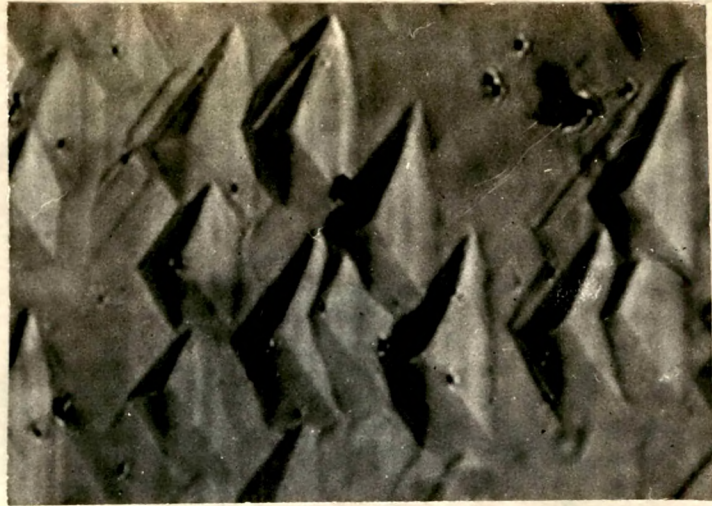


Fig. VI-1a

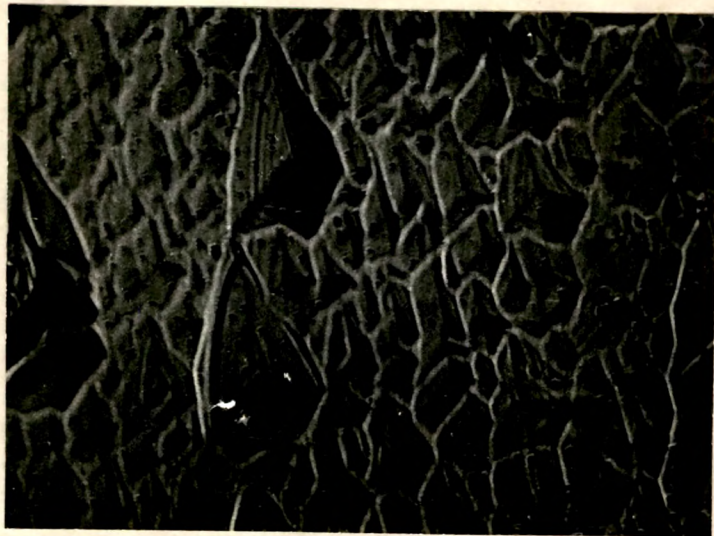


Fig. VI-1b

The etching was carried out in the Edward's Coating Unit, model 12EA/345. A tungsten filament was used. The crystal to be etched was kept on the filament, which was made into the shape of a boat. The temperature was measured by a thermometer which was kept in contact with the crystal and the filament. The etching was carried out at different temperatures and pressures.

Crystals were first etched under a vacuum less than 0.1μ of Hg at 100°C for 3 minutes. The point-bottomed pits that appeared had a characteristic shape as shown in Fig.VI.2. These pits are not symmetrical about the c-axis and one of the edges is parallel to the c-axis. The opposite edge does not have a definite and straight boundary. A few flat-bottomed pits are also seen. The point-bottomed pits are slightly eccentric. The pit density was of the order of $4 \times 10^4 / \text{cm}^2$.

On further etching the specimen for another 5 minutes, it is found that the pits enlarge and diffuse into each other leaving only a few large and complex pits as seen in Fig.VI.3. Some pits



Fig.VI-2

X450

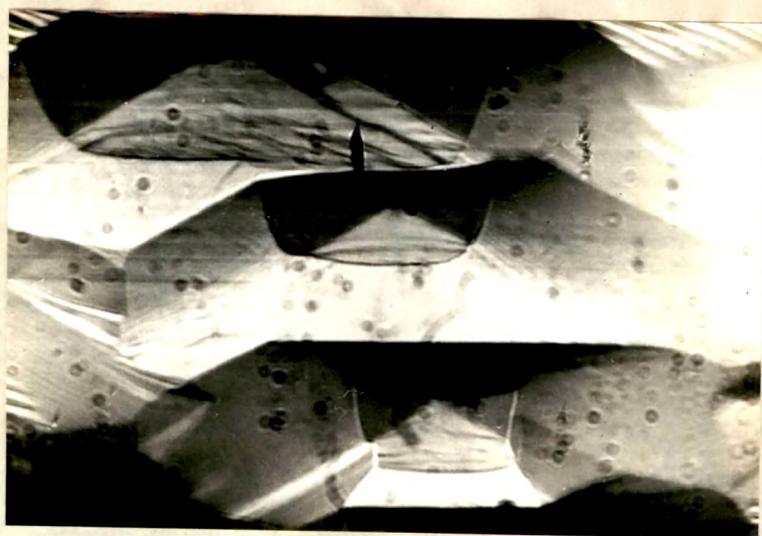


Fig.VI-3

X450

become terraced. The striated look on the crystal surface is due to the onset of general evaporation.

Fig.VI.4 is the surface of another crystal which has been etched for 1 minute at the same pressure and at a temperature of 120°C. The pits do not have a definite shape. It is noted that many of the etch pits are having a hole at the bottom indicating that they are at the sites of screw dislocations. To confirm this observation, the same specimen has been etched in sulphuric acid at a temperature of 100°C for 1 minute. From Fig.VI.5 it is seen that a chemical pit is formed at each point where there had been a thermal pit. It leads to the conclusion that thermal etch pits are formed at the sites of the emergence of dislocation lines.

Fig.VI.6 is another surface etched for 3 minutes at the same temperature and pressure. Here also the edges of the pits are not very clear, but the planes constituting them are clearly visible. The pit depth varies from 15 to 20 μ as measured by light-profile. On etching further for 10 minutes the size of the pits

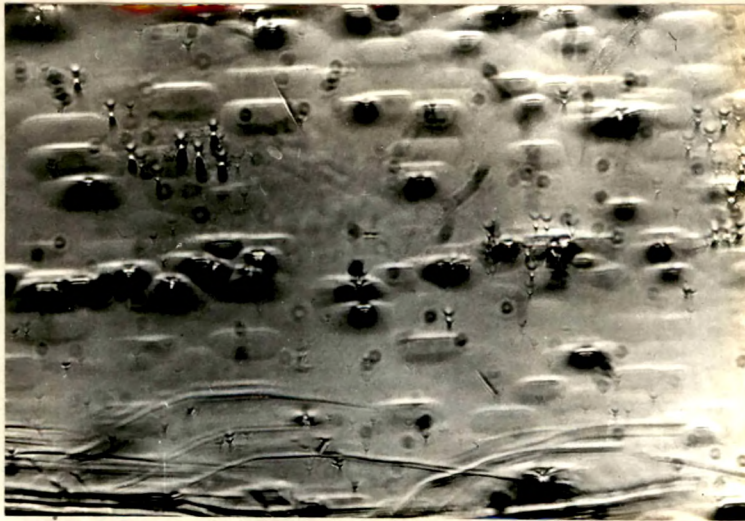


Fig.VI-4

X220



Fig.VI-5

X220

increases but the density remains the same, as seen from Fig.VI.7. Fig.VI.8 is the same surface after chemical etching. A chemical pit is seen at the centre of each pit and in certain cases more than one chemical pits are seen at the centre of a thermal pit. The edges become clearer. A probable reason for this would be that the planes constituting the pits are not attacked by H_2SO_4 whereas at the edges it is only slightly inclined to the prism plane and is dissolved by H_2SO_4 . A few pits are formed at other regions also as seen from Figs.VI.9 & 10. But no pit is formed on the planes constituting the pits except for the one plane which appears corroded. The same pattern of etching has been observed on etching the $(10\bar{1}1)$ rhombohedron face of the vapour grown Te crystal. Therefore it may be one of the $\{10\bar{1}1\}$ planes. Another thing that can be noted from Figs.VI.4 & 5 is that the edge parallel to c-axis in the case of a chemical pit is just the opposite to that which is parallel to c-axis in the case of thermal etch pit.

The temperature at which etching commences, has been found to be very sensitive to the pressure. As

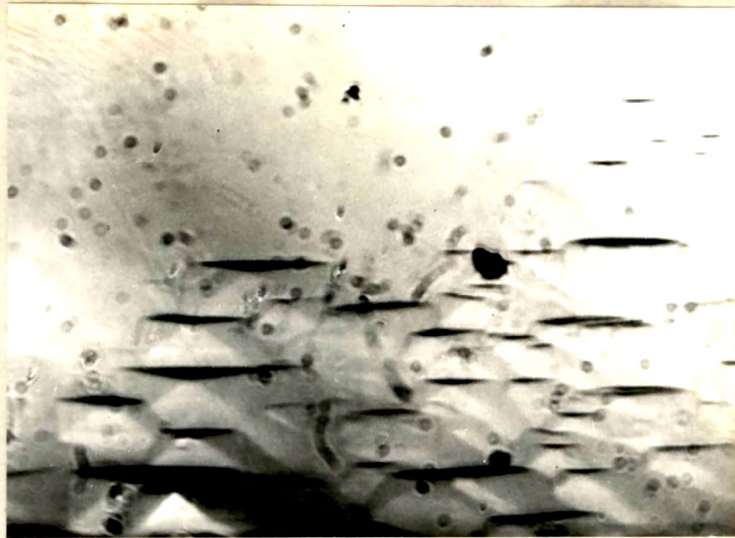


Fig.VI-6

X220



Fig.VI-7

X220



Fig.VI-8

X220



Fig.VI-9

X450

pressure increased the etching temperature also increased.

At atmospheric pressure evaporation sets in only above 320°C. No pit is observed. Only general evaporation takes place. A thin yellowish oxide layer is formed and this may be preventing the formation of etch pits. Etching for 10 minutes above 320°C leaves a very rough surface.

A specimen has been etched at a pressure of less than 0.01 mm of Hg. The temperature was slowly raised to see at which temperature the etching takes place. Etching starts at a temperature of 210°C. After etching for 5 minutes at 210°C elongated pits are obtained as seen from Fig.VI.11. The pit density is slightly higher than that in Fig.VI.2. It is about $11 \times 10^4 / \text{cm}^2$. As it is etched for a longer time the pit density decreases to about $6 \times 10^4 / \text{cm}^2$ and the pit size increases. Boat-shaped pits are obtained as seen from Figs VI.12 & 13. On etching further for a longer time, the point-bottomed pits become very deep and the flat-bottomed pits become over-imposed giving the surface a rough look. Fig.VI.14 is such a photomicrograph.

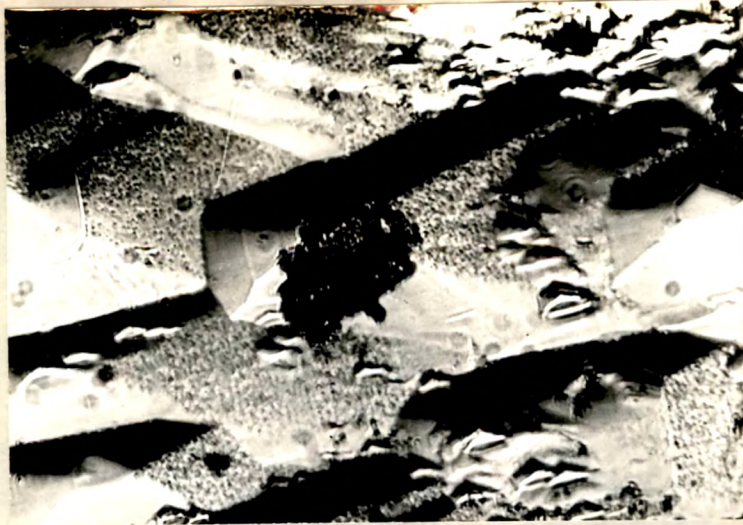


Fig.VI-10

X450



Fig.VI-11

X240

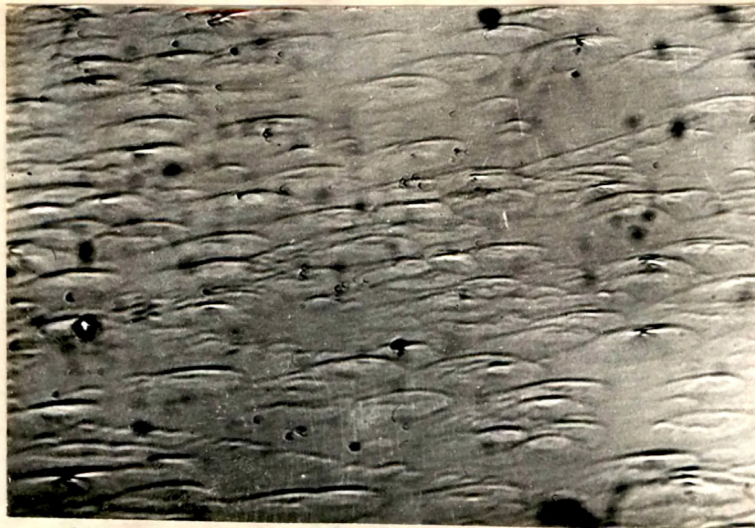


Fig.VI-12

X240



Fig.VI-13

X240

The pressure has been further reduced to less than 10μ . The etching sets in at about 170 to 180°C . Etching a specimen for 5 minutes gives boat-shaped pits as shown in Fig.VI.15. The pit density is in the same order as in other cases. Only one edge of the pit is sharp enough. Both point-bottomed and flat-bottomed pits are observed.

On etching the same specimen for another 5 minutes the pit size increases. Many of the flat-bottomed pits disappear and the point-bottomed pits become larger and deeper as seen in Fig.VI.16. A hole is seen at the centre of each point-bottomed pit which shows that they are at sites of emergence of screw dislocations of large Burgers vectors. The specimen has been etched for a total time of 25 minutes. All the flat-bottomed pits disappear and the point-bottomed pits take the form as shown in Fig.VI.17. The shape of the pits is very much like the pits formed at a pressure less than 0.1μ . At a pressure less than 1μ also the dislocations can be revealed by etching at a lower temperature.

Another specimen has been etched in the electron-microscope chamber and was observed under reflection

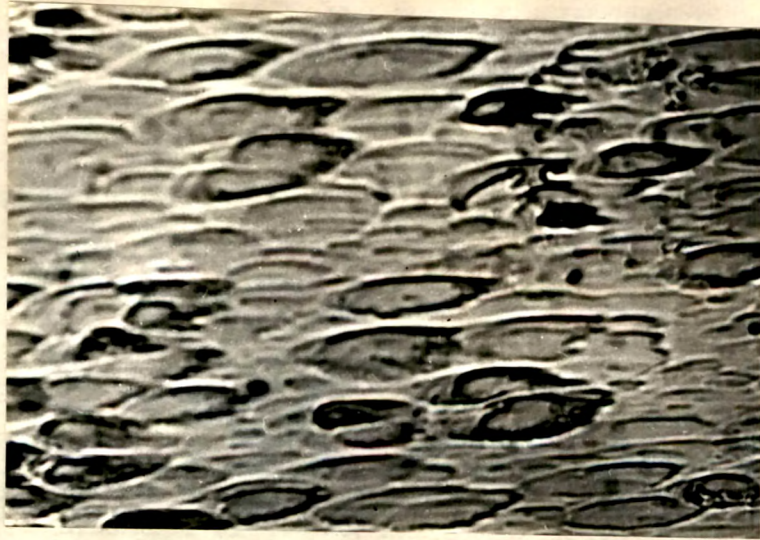


Fig.VI-14

X240



Fig.VI-15

X170



Fig.VI-16

X215



Fig.VI-17

X215

set-up. Fig.VI.18 is the surface before etching. The scratch seen in the picture was produced while fixing up the specimen in the specimen-holder. Fig.VI.19 is the same surface after etching for 30 seconds at a temperature of 120°C. The pit shape is the same as that in the case of those specimens etched in the coating unit. Fig.VI.20 is the same surface after a further etching of 30 seconds. The pit size is increased considerably and it is seen that two or more pits join to form a large pit. All the individual pits can be seen inside a common boundary. The specimen was etched for a total time of $1\frac{1}{2}$ minutes. The pit size increases considerably. Some pits become terraced as seen from Fig.VI.21. Individual pits have the same shape as those in Fig.VI.2. But the larger pits which are constituted of more than one pit have a well-defined rectangular shape. When the specimen was etched for $2\frac{1}{2}$ minutes the crystal melted slowly and re-crystallization takes place as shown in Fig.VI.22.

From the above studies, it is found that thermal etching of Te can be carried out at different pressures and different temperatures. As the order of vacuum



Fig.VI-18

X1500



Fig.VI-19

X1500



Fig. VI-20

X1500



Fig. VI-21

X1500



Fig.VI-22

X1500

increases the temperature at which etching can be carried out conveniently, decreases. The time of etching increases at higher pressures. Or, in other words, as pressure increases the rate of etching decreases. The etching rate is the highest at the lowest pressure and the etching temperature is the lowest at the lowest pressure.

A few cleaved specimens have also been etched in the coating unit at a vacuum of the order of 0.1μ . The specimens have been cleaved at liquid nitrogen temperature. Etching for 5 minutes a surface as seen in Fig.VI.23 is obtained. The deformed layer is evaporated off in the first place and pits slowly appear in the background, just as lines along the cleavage steps. Etching for another 5 minutes, the cleavage steps and the deformed layer disappear and the pits are enlarged. Fig.VI.24 is the photomicrograph of the same surface. The pits do not have sharp edges. An etch groove is also seen, on the left hand corner of the photograph. A prolonged etching makes the surface rough and the pits are very much enlarged. A row of pits along a slip line is seen in Fig.VI.25.

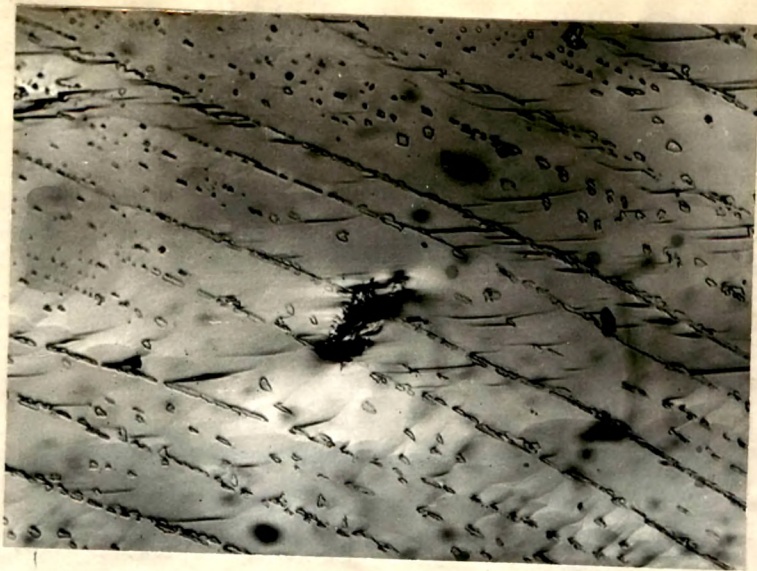


Fig.VI-23

X170



Fig.VI-24

X170



Fig.VI-25

X210

The advantage of thermal etching in the case of cleaved specimens is that it is not necessary to do ~~chemical~~ polishing to remove the deformed layer, and thus avoids the formation of films on the surface and the introduction of more dislocations.

CONCLUSIONS:

- (1) Thermal etching can be successfully employed to reveal dislocations on $\{10\bar{1}0\}$ faces of Te.
- (2) All the pits produced at lower vacuums and higher temperatures do not correspond to dislocations.
- (3) The pits are eccentric and assymmetric about the c-axis. One edge is parallel to c-axis.
- (4) As the order of vacuum increases the etching temperature decreases and the rate of etching increases.
- (5) At vacuums of the order of less than $10\ \mu$ upto $0.1\ \mu$ etching rate can be controlled. At still higher vacuums it becomes difficult to control the etching rate.

- (6) The shape of the etch pits are different at lower vacuum and higher vacuum. As the order of vacuum changes the pit shape also slightly changes i.e. the etching rates. V_s and V_n change with pressure.
- (7) The deformed layer that appears on cleavage surfaces are evaporated away leaving a clean and smooth surface for the dislocation studies.
- (8) Array of thermal etch pits along dislocation lines, the presence of pits with a hole at the bottom and the formation of chemical etch pits, when etched with H_2SO_4 , at the sites of thermal pits show that the pits are produced at the sites of dislocations.
- (9) One disadvantage of thermal etching is that, on a fairly etched surface sometimes it becomes difficult to count the pit density as two or more pits may join together to form a big pit.
- (10) It is not possible to determine the positive directions of the axes of the crystal from thermal etch pits.

REFERENCES

1. Chalmers, B., (1948) Proc. Roy. Soc., A193, 465.
King, R. and
Shuttleworth.
2. Hendrickson, A.A. (1955) Acta Met., 3, 64.
and Machlin, E.S.
3. Moore, A.J.W. (1958) Acta Met., 6, 293.
4. Hendros, E.D. and (1959) Acta Met., 7, 521.
Moore, A.J.W.
5. Hirth, J.P. and (1958) J. Appl. Phys., 29, 595.
Vassamillet, L.
6. Mullins, W.W. (1957) J. Appl. Phys., 28, 333.
7. Lowe, R.M. (1964) Acta Met., 12, 1111.
8. Danilov, V.N. (1962) Sov. Phys. Cryst., 7, 127.
9. Sagar, A. and (1966) Praktische Metallographic,
Faust, J.W. Jr. 1, 27.
10. Patel, A.R. and (1965) Surface Science, 4, 502.
Agarwal, M.K.
11. Patel, A.R. and (1969) Jap. J. Appl. Phys.,
Chaudhari, R.M. 8, 667, 672.
12. Votava, E. and (1959) Acta Met., 7, 392.
Bregheza, A.
13. Ponelet, E. and (1964) Acta Met., 12, 593.
Bariany, D.
14. Young, F.W. Jr. (1956) J. Appl. Phys., 27, 559.

15. Young, F.W. and Gwathmey, A.T. (1960) J.Appl.Phys., 31, 225.
16. Fraser, M.A., Caplan, D. and Barr, A.A. (1956) Acta Met., 4, 186.
17. Booker, G.R. and Valdre, V. (1966) Phil Mag., 13, 421.
18. Dunn, C.G. and Walter, J.L. (1959) Acta Met., 7, 648.
19. Larventev, F.F., Soifer, L.M. and Startser, V.I. (1960) Sov.Cryst., 5, 449.
20. Thakkar, B.B. (1967) Ph.D.Thesis, M.S.Univ. of Baroda.
21. Ellis, S.G. (1955) J.Appl.Phys., 26, 1140.
22. Lovell, L.C., Wernick, J.H. and Benson, K.E. (1958) Acta Met., 6, 716.
23. Blum, A.I. (1960) Fizika Tverdogo Tela, 2, 1666.
24. Blakemore, J.S., Schultz, J.W. and Nomura, K.C. (1960) J.Appl.Phys., 31, 2226.
25. Blakemore, J.S. and Nomura, K.C. (1961) J.Appl.Phys., 32, 745.
26. A. Koma, E. Tatimoto, and S. Tanaka. (1970) Phys. Stat. Sol., 40, 239.
27. Shukla, R.K. (1970) Ph.D. Thesis, M.S.Univ. of Baroda.